

Two-dimensional Microwave Tomographic Imaging of Breast Tissues

¹G. Bindu, ²Santhosh John Abraham, ¹Anil Lonappan,
¹Vinu Thomas, ¹C.K. Aanandan and ¹K.T. Mathew

¹Microwave Tomography and Materials Research Laboratory, Department of Electronics,
Cochin University of Science and Technology, Kochi-682 022, India

²Department of Surgery, Lourde Hospital, Cochin, India

Abstract: Despite its recognized value in detecting and characterizing breast disease, X-ray mammography has important limitations that motivate the quest for alternatives to augment the diagnostic tools that are currently available to the radiologist. The rationale for pursuing electromagnetic methods are based on the significant dielectric contrast between normal and cancerous breast tissues, when exposed to microwaves. The present study analyzes two-dimensional microwave tomographic imaging on normal and malignant breast tissue samples extracted by mastectomy, to assess the suitability of the technique for early detection of breast cancer. The tissue samples are immersed in matching coupling medium and are illuminated by 3 GHz signal. 2-D tomographic images of the breast tissue samples are reconstructed from the collected scattered data using distorted Born iterative method. Variations of dielectric permittivity in breast samples are distinguishable from the obtained permittivity profiles, which is a clear indication of the presence of malignancy. Hence microwave tomographic imaging is proposed as an alternate imaging modality for early detection of breast cancer.

Key words: Microwave imaging, breast cancer detection, permittivity, inverse scattering

Introduction

Breast cancer affects many women and early detection aids in fast and effective treatment. X-ray mammography is currently the most effective imaging method for detecting clinically occult breast cancer. However, despite significant progress in improving mammographic techniques for detecting and characterizing breast lesions, mammography reported high false-negative rates (Huynh *et al.*, 1998) and high false-positive rates (Elmore *et al.*, 1998). These difficulties are attributed to the intrinsic contrast between normal and malignant tissues at X-ray frequencies. In X-ray tomography a tissue is differentiated based on density. However in most cases, tissue density does not depend on tissue physiological state. Important tissue characteristics such as temperature, blood content, blood oxygenation and ischemia cannot be differentiated by X-ray tomography. For soft tissues like human breast, X-ray cannot image the breast anomalies at an early stage, as there is no significant variation in density between normal and malignant breast tissues (Fear *et al.*, 2000).

Microwave imaging is a new technology, which has potential applications in the field of diagnostic medicine (Fear *et al.*, 2002a, b). The basic motivation for this is improved physiologic

Corresponding Author: K.T. Mathew, Microwave Tomography and Materials Research Laboratory,
Department of Electronics, Cochin University of Science and Technology, Kochi-682 022, India
Tel: 91 484 2576418 Fax: 91 484 2575800

and pathophysiologic correlation, especially in soft tissue. This expectation is based on the molecular (dielectric) rather than atomic (density) based interactions of the microwave radiation with the target when compared with X-ray imagery. When exposed to microwaves, the high water content of malignant breast tissues cause significant microwave scattering than normal fatty breast tissues that have low water content. It is reported that dielectric permittivity and conductivity increase for cancerous breast tissue is three or more times greater than the host tissue (Chaudhary *et al.*, 1981). Due to the improved dielectric contrast, better tissue characterization too is possible.

Microwaves can be used effectively for the detection of biological anomalies like tumor at an early curable stage itself. At microwave frequencies the sensitivity, specificity and the ability to detect small tumors is the dielectric contrast between normal and malignant breast tissues (Semenov *et al.*, 1996). Malignant breast tissues exhibit considerable increase in bound water content compared to the normal tissues and hence a high value of permittivity. When exposed to microwaves, the high water content of malignant breast tissues cause significant microwave scattering than normal fatty breast tissues that have low water content.

Some benign tumors too respond to microwaves similar to that of malignant tumors (Rangayyan *et al.*, 1997). However, characterizing and analyzing such benign tumors is not considered in this study.

Many prototypes of active microwave imaging has been reported by Semenov *et al.* (1996) and Meaney *et al.* (2000). The need for using suitable coupling medium, to enhance the coupling of electromagnetic energy to the object as well as to increase the resolution is emphasized (Meaney *et al.*, 2003). A suitable coupling medium accomplishes wavelength contraction without propagation loss penalty associated with increased frequency. In near field microwave medical imaging environment, resolution is determined by the aperture dimensions of the antenna, which can be generalized to far field by using a suitable coupling medium. A contrast in the dielectric properties of the object and the coupling medium decreases the measurement accuracy, increases the attenuation, creates temperature drifts and unpredictable local temperature gradients (Foti *et al.*, 1986).

This study analyzes two-dimensional microwave tomographic imaging as an alternate imaging modality for early detection of breast cancer. Microwave studies are performed on normal and malignant breast tissues in the presence of a matching coupling medium. The reconstructed 2-D tomographic images from the collected fields show that microwave tomographic imaging could detect breast cancer with a high rate of accuracy.

Materials and Methods

The study was performed at the Microwave Tomography and Materials Research Laboratory of the Department of Electronics, Cochin University of Science and Technology, Cochin, India. Breast tissue samples for the study were collected from Department of Surgery, Lourde Hospital, Cochin, within 30 min of mastectomy.

System Configuration

The designed prototype of 2-D microwave imaging is shown in Fig. 1. The breast sample supported on a PVC holder is mounted on a circular platform capable of circular motion in the horizontal plane. The platform along with samples is kept inside a tomographic chamber of radius 12 cm and height 30 cm, coated inside with suitable absorbing material. The chamber is filled with coupling medium. Suspended bowtie antennas are used for both transmission and reception of

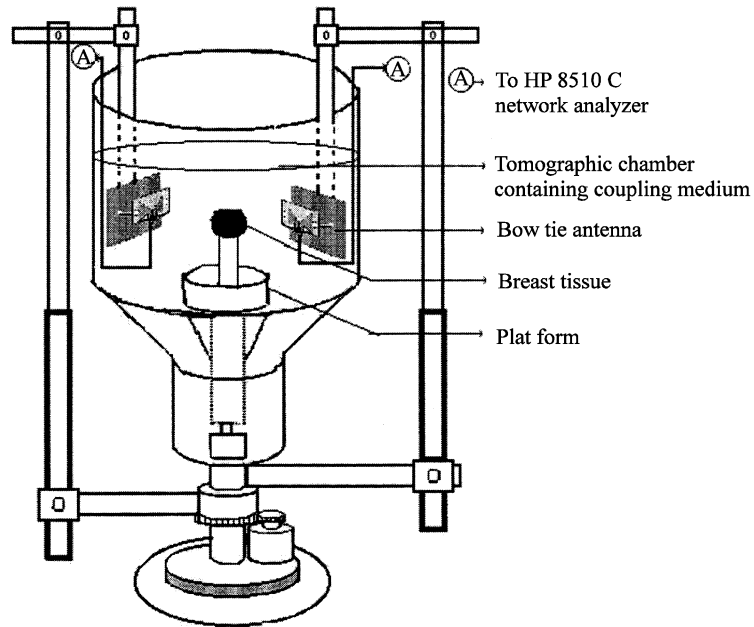


Fig. 1: Experimental setup

microwave energy. All measurements are done using HP 8510 C network analyzer; interfaced with Compaq work station SP 750 using GPIB bus.

Coupling Medium

The coupling medium used here is corn syrup. Dielectric parameters of the material in the frequency range of 2-4 GHz are done using cavity perturbation technique (Bindu *et al.*, 2004a, Mathew and Rareendranth, 1999). This frequency range is adopted, as the resonant frequency of the antenna used in our microwave imaging studies is 3 GHz. Also it conveniently includes the Industrial Scientific and Medical (ISM) applications band of 2450 MHz. The dielectric permittivity and conductivity variations of corn syrup in the frequency range of 2-4 GHz are shown in Fig. 2. It is observed that for corn syrup, the dielectric permittivity decreases and conductivity increases, with the increase of frequency. This result coincides with the studies on dielectric properties of biological tissues (Gabriel *et al.*, 1996).

The complex permittivity of the medium can be written as

$$\epsilon_r = \epsilon_r' - j \epsilon_r'' \quad (1)$$

where ϵ_r' is the dielectric permittivity and ϵ_r'' is the dielectric loss of the medium

The loss tangent

$$\tan \delta = \epsilon_r'' / \epsilon_r' \quad (2)$$

The propagation constant

$$\gamma = \sqrt{j\omega\mu_0(\sigma + j\omega\epsilon)} = \alpha + j\beta \quad (3)$$

where α represents the attenuation factor and β the phase factor. The conductivity σ is given by

$$\sigma = \omega \epsilon_0 \epsilon_r'' \quad (4)$$

Substituting Eq. 1, 2 and 4 in 3 and simplifying, we get

$$\alpha = 2\pi f \sqrt{\mu_0 \epsilon_0 \epsilon_r'} \left[\sqrt{1 + \tan^2 \delta} - 1 \right] \quad (5)$$

and

$$\beta = 2\pi f \sqrt{\mu_0 \epsilon_0 \epsilon_r'} \left[\sqrt{1 + \tan^2 \delta} + 1 \right] \quad (6)$$

If the wave is considered traveling in the + z direction, $e^{-\alpha z}$ represents the decaying envelope of the wave and $e^{-j\beta z}$ represents the sinusoidal nature of the wave whose phase is βz . The total loss encountered by the wave over a distance z consists of dissipation loss L_{diss} due to conduction currents being excited in the medium and diffusion loss L_{diff} due to the spherical spreading of energy (Foti *et al.*, 1986).

They are given by,

$$L_{diss} = 20 \log_{10} e^{\alpha z} \quad (7)$$

$$L_{diff} = 20 \log_{10} (\beta z) - 29.14(\text{dB}) \quad (8)$$

Hence the total loss

$$L_{total} = L_{diss} + L_{diff} \quad (9)$$

Table 1: Propagation loss parameters of water, corn syrup and saline at 3 GHz at a distance of 12 cm from the transmitter

Sample	Total loss dB	
	Dissipation loss	+ Diffusion loss
Corn syrup	10.7	
Water	180	
Saline (0.5% NaCl)	165	

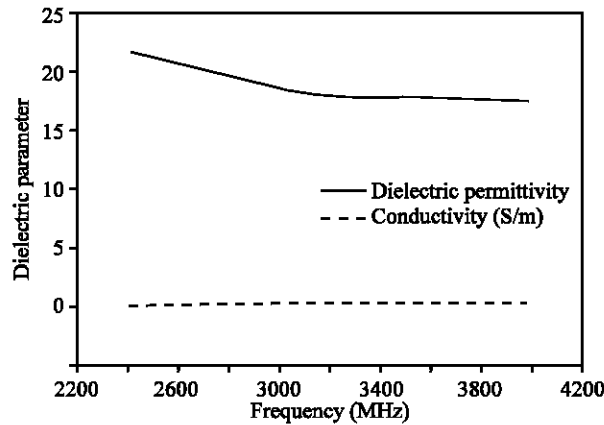


Fig. 2: Variation of dielectric permittivity and conductivity for corn syrup

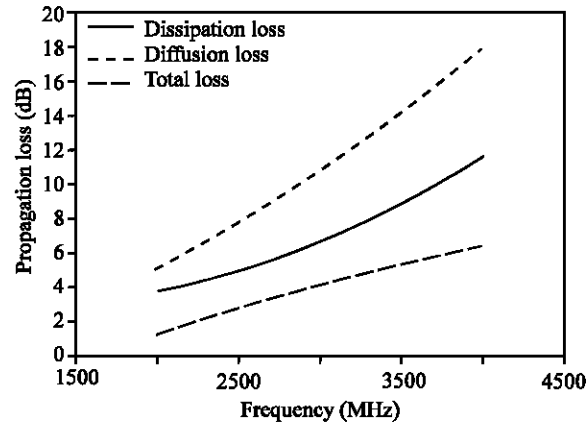


Fig. 3: Propagation loss characteristics of corn syrup

Figure 3 shows the propagation loss characteristics of corn syrup. It is seen that losses increase with frequency, which is due to the increase of conductivity. Table 1 compares the loss parameters of distilled water and saline (Foti *et al.*, 1986) with corn syrup at 3 GHz, at a distance of 12 cm from the transmitter. The loss values are acceptable when compared to the loss parameters of conventional coupling medium like distilled water and saline (Foti *et al.*, 1986). It is reported that in water the rate of increase of loss vs. distance is much higher due to the dominant dissipation loss.

Antenna Design

Coplanar strip line fed bowtie antennas generating TM_{01} mode are designed for both transmission and reception of microwave signals. The experimental investigation (Bindu *et al.*, 2004b,c) shows that the designed antenna, in air, exhibits a center frequency of 3 GHz, enhanced 2:1 VSWR bandwidth of ~ 46% in the operational band of 1.850-3.425 GHz and a return loss of -53 dB. In corn syrup, the bandwidth is enhanced to 91% in the range of 1.215-3.810 GHz with resonant frequency of 2.855 GHz and return loss of -41 dB. Figure 4 a and b show the radiation characteristics of the antenna. It is observed from the figures that the antenna exhibits maximum forward radiation and less back radiations at 3 GHz.

Samples

Samples of breast tissues of four patients are subjected to the study. Cancerous tissue of ~ radius 0.5 cm inserted in normal tissue of ~ radius 1 cm, of patient 1, is taken as sample 1. Samples 2 and 3 consists of four tumorous inclusions of ~ radius 0.25 cm each inserted in normal tissue of ~ radius 1 cm, of patients 2 and 3. Scattered inclusions of cancerous tissue of ~ radius 0.1 cm each inserted in normal tissue, of patient 4 is treated as sample 4. The samples are supported on a cylindrical PVC holder ($\tan \delta = 0.0018$ and $\epsilon_r = 2.4$ at 3 GHz) of height 15 cm at the center of the measurement set up as shown in Fig. 1.

2-D Microwave Tomographic Imaging

The problem of microwave tomographic imaging has been a topic of theoretical and experimental study for many years. Several research groups are investigating microwave tomography for breast cancer detection (Meaney *et al.*, 1996, 1998, Dun Li *et al.*, 2004, Bulyshev *et al.*, 2001).

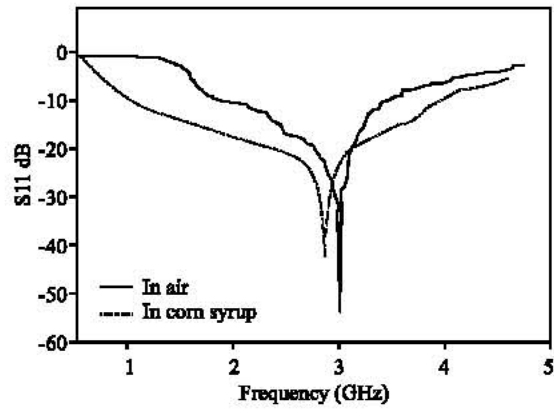


Fig. 4a: Radiation characteristics of bowtie antenna

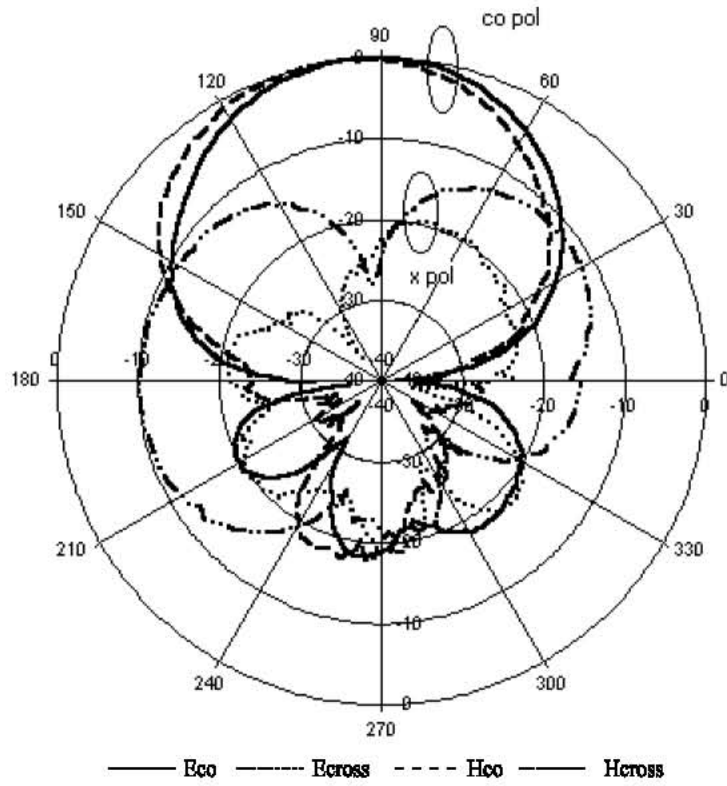


Fig. 4b: Radiation pattern of the antenna measured at 3 GHz

Data Acquisition

For data acquisition, the breast sample is illuminated by bow-tie antenna at a frequency of 3 GHz. As shown in Fig. 1, the transmitting antenna is fixed at a radius of 6 cm on the circular rail, while the receiving antenna is rotated around the object at 6 cm radius. The platform upon which the sample is mounted is rotated from 0° to 360° in steps of 10° and the receiving antenna is rotated from 30° to 330° in steps of 10°. For every 10° rotation of the platform with the sample, the receiving antenna makes the measurement in steps of 10°.

Reconstruction Algorithm

The contrast in the dielectric properties of the object creates multiple scattering of the wave inside the object. This poses a non linear inverse scattering problem which is formulated in terms of Fredholm integral equation of the second kind (Taflove, 1998). The object is considered inhomogeneous in the xy plane but homogeneous in the z direction. For an incident TM wave, the total electric field at the receiver (Taflove, 1998) is given by,

$$\phi(\mathbf{r}) = \phi_{\text{inc},b}(\mathbf{r}) + \omega^2 \mu \int_{\mathcal{V}} dS g_b(\mathbf{r}, \mathbf{r}') \delta\epsilon(\mathbf{r}') \phi(\mathbf{r}') \quad (10)$$

where \mathbf{r} stands for a point in the measurement domain and \mathbf{r}' for the object domain. $\phi_{\text{inc},b}(\mathbf{r})$ is the incident field in the presence of the background inhomogeneity and the integral term is the scattered field due to the dielectric contrast between the scatterer and the background medium.

$$\delta\epsilon(\mathbf{r}') = \epsilon(\mathbf{r}') - \epsilon_b(\mathbf{r}') \quad (11)$$

is called as the object function, $g_b(\mathbf{r}, \mathbf{r}')$ the Green's function and $\phi(\mathbf{r}')$ the total electric field inside the scatterer. Equation 10 is used for both the forward and inverse solutions. In the forward problem, both the medium properties and the domain of inhomogeneity are known and the equation is solved to obtain the total electric field. In the inverse problem, scattered fields are measured at discrete points and the medium properties are the unknowns to be determined. The problem is linearized using distorted Born approximation (Chew *et al.*, 1990) by replacing $\phi(\mathbf{r}')$ with $\phi_{\text{inc},b}(\mathbf{r})$. As the background medium is inhomogeneous, Green's function is solved numerically (Richmond, 1965). Discretization of the integral equation in the inverse problem yields vector representations of the scattered field and the object profile. As the inverse problem is ill posed, a regularization procedure (Taflove, 1998; Chew *et al.*, 1990) is employed where an optimization technique is adopted to minimize the error by minimizing a cost functional. The non-uniqueness and instability of the problem is thus circumvented and an adequate solution is provided. The obtained $\delta\epsilon$ is used to improve $\epsilon_b(\mathbf{r})$ which in turn is used to update the parameters in Eq. 10. The iteration is continued until convergence is reached. The imaging area is restricted to 16 x 16 pixels due to computational complexity. The sampling rate considered is 0.1λ .

Results and Discussion

Corn syrup sample of dielectric permittivity and conductivity as 18.7 and 0.64 S/m at 3 GHz is used as the coupling medium in this study. In order to check the compatibility of corn syrup with breast tissue samples, dielectric properties of the breast tissue samples are measured using cavity perturbation technique and are compared with that of the corn syrup at a frequency of 3 GHz.

Table 2: Dielectric parameters of breast tissue samples and corn syrup measured using cavity perturbation technique at 3 GHz

Sample		Dielectric permittivity	Conductivity (S/m)
Breast tissue, Patient 1	Normal	24.82	1.21
	Cancerous	32.31	1.95
Breast tissue, Patient 2	Normal	18.85	0.72
	Cancerous	38.73	2.25
Breast tissue, Patient 3	Normal	19.98	0.92
	Cancerous	39.50	2.33
Breast tissue, Patient 4	Normal	23.70	1.15
	Cancerous	29.20	1.37
Corn syrup		18.7	0.64

Table 3: Dielectric parameters and loss factors of corn syrup with frequency

Frequency (GHz)	Dielectric permittivity	Conductivity (S/m)	Total loss (dB)
2.428	22.5	0.59	6.85
2.675	20.23	0.61	8.83
2.985	18.7	0.67	10.70
3.265	18.2	0.69	11.40
3.654	17.5	0.71	13.80
3.983	17.3	0.72	17.50

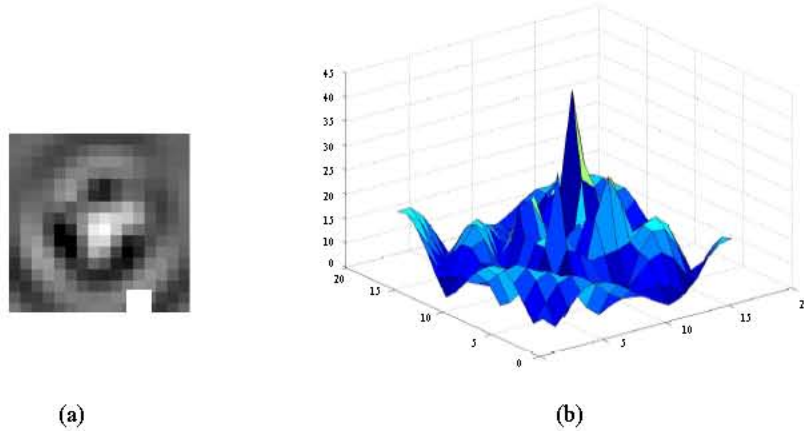


Fig. 5: Sample 1-a) 2D microwave tomographic image. b) Dielectric permittivity profile

Table 2 shows the comparison. The measured dielectric parameters of breast tissues match with the literature data too (Chaudhary *et al.*, 1981, Campbell *et al.*, 1992). When corn syrup is used as coupling medium for imaging normal breast tissue with cancerous inclusion, good resolution is achieved as the dielectric permittivity of corn syrup matches with that of the normal breast tissue as seen in Table 2. As the conductivity of the medium is less than that of the actual tissue sample, loss tangent decreases and hence the propagation loss. Table 3 shows the tabulated form of the graphs shown in Fig. 2 and 3. The frequencies mentioned in the table are the resonant frequency of the cavity used in the cavity perturbation study.

The reconstructed 2-D tomographic images for the breast samples 1-4 are shown in Fig. 5-8. The dielectric contrast of the samples is clearly distinguishable from the images as well as from the permittivity profiles. Samples 1-3 are having ~ circular cross section without any cover, where as

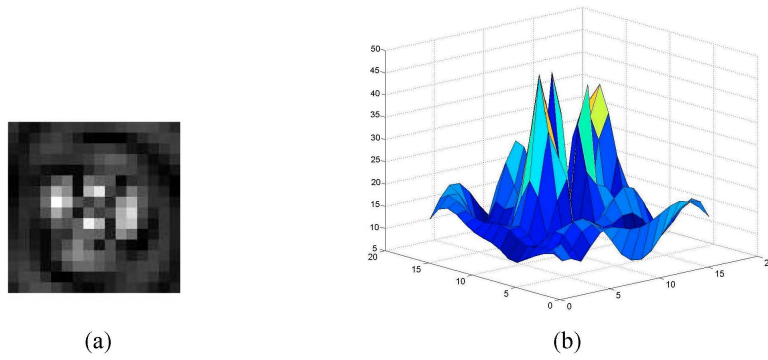


Fig. 6: Sample 2-a) 2 D microwave tomographic image. b) Dielectric permittivity profile

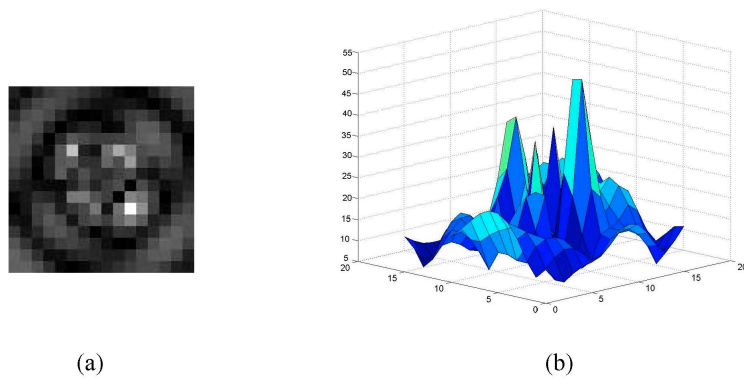


Fig. 7: Sample 3-a) 2 D microwave tomographic image. b) Dielectric permittivity profile

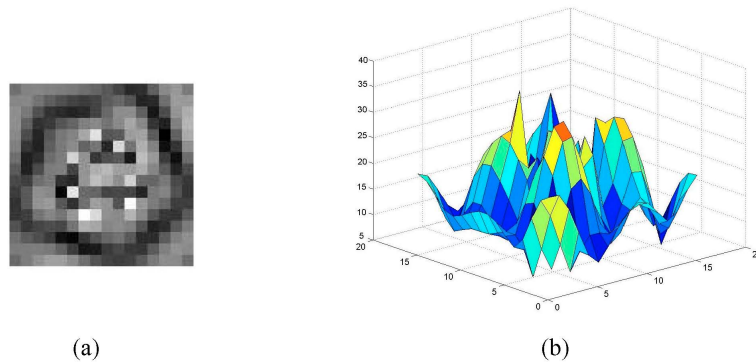


Fig. 8: Sample 4-a) 2 D microwave tomographic image. b) Dielectric permittivity profile

sample 4 is covered in a thin conical polythene study. This is done to check whether the shape of the sample too is reconstructed properly. As the dielectric permittivity of the coupling medium and the normal breast tissue samples are in good match, the tumor inclusions are clearly visible in Fig. 5-8. In Fig. 8, the shape of the sample too is reconstructed and is seen with a black border. This is due to the fact that polythene paper exhibits a very low permittivity of ϵ_r' 2.2 at 3 GHz. Scattered tumor inclusions are clearly distinguishable in the image. A resolution of 2 mm is achieved in this reconstruction with the use of corn syrup as the coupling medium. A comparison of the obtained permittivity values of the breast samples from Fig. 5-8 with that measured using cavity perturbation technique reported in Table 2 shows good agreement.

Sources of Error and Accuracy Conditions

Early stage tumor detection is the attractive feature of the proposed microwave medical imaging. So care is taken to eliminate all possible types of errors. In the present study HP 8510 network analyzer is used. Accuracy of this instrument is 0.001 dB for power measurement, 1 Hz for frequency measurement (HP 8510C Manual, 1988). Main sources of experimental errors are 1) Edge reflections from the antenna: The FDTD computed end-reflections observed at the feed point of the bowtie antenna relative to the exciting pulse is as low as -24 dB. 2) Reflections from the sample holder: The tissue samples are supported on a low loss PVC pipe having loss tangent ($\tan \delta$) 0.002. Hence reflections are negligible. 3) Medium reflections: As the tumor under study is immersed in a matching coupling medium, reflections are minimized and good resolution of the reconstructed image is ensured. 4) Error in using distorted Born approximation to linearize the inverse scattering problem: This method is adopted to reduce the computational complexity. Acceptable values of permittivity profiles are obtained with in vitro breast studies. The matter has to be further investigated with strong scatterers and fast forward iterative solvers. 5) Convergence: To ensure that global convergence is achieved, we performed five iterations and the same profile as with the fourth iteration was obtained.

Conclusions

Microwave tomographic imaging is explored as an imaging modality for early detection of breast cancer. In vitro studies on normal and malignant breast tissues suggest that microwave tomographic imaging could satisfactorily image the tissues showing clear discrimination in terms of dielectric permittivity. The presence of breast cancer can be easily determined by analyzing the dielectric permittivity profiles, as cancerous tissues exhibit higher value of dielectric permittivity compared to normal tissues even at early curable stage itself. This is an advantage of the technique compared with conventional X-ray mammography. Hence microwave imaging can be considered for early stage breast cancer detection.

Acknowledgement

Authors G. Bindu and Anil Lonappan thankfully acknowledge Council of Scientific and Industrial research, Govt. of India for providing Senior Research Fellowships.

References

- Bindu, G., A. Lonappan, V. Thomas, V. Hamsakutty, C.K. Aanandan and K.T. Mathew, 2004a. Microwave characterization of breast phantom materials. *Microwave and Optical Technol. Lett.*, 43: 506-508.
- Bindu, G., A. Lonappan, V. Thomas, V. Hamsakutty, C.K. Aanandan and K.T. Mathew, 2004b. Wideband bowtie antenna with coplanar stripline feed. *Microwave and Optical Technol. Lett.*, 42: 222-224.
- Bindu, G., A. Lonappan, C.K. Aanandan and K.T. Mathew, 2004c. Wideband bowtie antenna for confocal microwave imaging. *Asia Pacific Microwave Conference 2004 New Delhi India APMC 04/C/449*, 2004.
- Bulyshv, A.E., S.Y. Semenov, A.E. Souvorov, R.H. Svenson, A.G. Nazarov, Y.E. Sizov and G.P. Tatsis, 2001. Computational modeling of three-dimensional microwave tomography of breast cancer. *IEEE Trans. Biomed. Eng.*, 48: 1053-1056.
- Campbell, A.M. and D.V. Land, 1992. Dielectric properties of female human breast tissue measured *in vitro* at 3.2 GHz. *Phy. Med. Biol.*, 37: 193-210.
- Chaudhary, S.S., R.K. Mishra, A. Swarup and J.M. Thomas, 1981. Dielectric properties of normal and malignant human breast tissues at radiowave and microwave frequencies. *Ind. J. Biochem. Biophys.*, 21: 76-79.
- Chew, W.C. and Y.M. Wang, 1990. Reconstruction of two-dimensional permittivity distribution using the distorted born iterative method. *IEEE Transactions on Medical Imaging*, 9: 218-225.
- Dun, Li, P.M. Meaney, T. Raynolds, S. Pendergrass, M. Fanning and K.D. Paulsen, 2004. A parallel-detection microwave spectroscopy system for breast imaging. *Rev. Sci. Inst.*, 75: 2305-2313.
- Elmore, J.G., M.B. Barton, V.M. Mocerri, S. Polk, P.J. Arena and S.W. Fletcher, 1998. Ten year risk of false positive screening mammography and clinical breast examinations. *New England J. Med.*, 338: 1089-1096.
- Fear, E.C. and M.A. Stuchly, 2000. Microwave detection of breast cancer. *IEEE Trans. Microwave Theory and Techniques*, 48: 1854-1863.
- Fear, E.C., S.C. Hagness, P.M. Meaney, M. Okoniewski and M.A. Stuchly, 2002a. Enhancing breast tumor detection with near field imaging. *IEEE Microwave Magazine*, 3: 48-56.
- Fear, E.C., L. Xu, S.C. Hagness and M.A. Stuchly, 2002b. Confocal microwave imaging for breast cancer detection: Localization of tumors in three dimensions. *IEEE Trans. Biomed. Eng.*, 49: 812-821.
- Foti, S.J., R.P. Flam, J.F. Aubin, L.E. Larsen and J.H. Jacobi, 1986. A Water Immersed Microwave Phased Array System for Interrogation of Biological Targets in Medical Applications of Microwave Imaging. *IEEE Press New York*, pp: 148-166.
- Gabriel, S., R.W. Lau and C. Gabriel, 1996. Dielectric properties of biological tissues:II. Measurements in the frequency range 10 Hz to 20 GHz. *Phys. Med. Biol.*, 41: 2251-2269.
- HP 8510C Network Analyzer Operating and Programming Manual, 1988 Hewlett-Packard.
- Huynh, P.T., A.M. Jarolimek and S. Dayee, 1998. The false-negative mammogram. *Radiographics*, 18: 1137-1154.
- Mathew, K.T. and U. Raveendranath, 1999. *Sensors Update*. Wiley-VCH Germany, pp: 185-210.

- Meaney, P.M., K.D. Paulsen, A. Hartov and R.K. Crane, 1996. Microwave imaging of tissue assessment: Initial evaluation in multitarget tissue equivalent phantoms. *IEEE Trans. Biomed. Eng.*, 43: 878-890.
- Meaney, P.M., Keith D. Paulsen and John T. Chang, 1998. Near-field microwave imaging of biologically based materials using a monopole transceiver system. *IEEE Trans. Microwave Theory and Techniques*, 46: 31-44.
- Meaney, P.M., M.W. Fanning, Dun Li, S.P. Poplack and K.D. Paulsen, 2000. A clinical prototype of active microwave imaging of the breast. *IEEE Trans. Microwave Theory and Techniques*, 48: 1841-1853.
- Meaney, P.M., S.A. Pendergrass, M.W. Fanning, Dun Li and K.D. Paulsen, 2003. Importance of using reduced contrast coupling medium in 2D microwave breast imaging. *J. Electromagnetic Waves and Application*, 17: 333-355.
- Rangayyan, R.M., N.M. El-Faramawy, J.E.L. Desautels and O.A. Alim, 1997. Measures of acutance and shape for classification of breast tumor. *IEEE Trans. Med. Imaging*, 16: 799-810.
- Richmond, J.H., 1965. Scattering by a dielectric cylinder of arbitrary cross section shape. *IEEE Trans. Antennas and Propagation*, 13: 334-341.
- Semenov, S.Y., R.H. Svenson, A.E. Souvorov, V.Y. Borisov, Y. Sizov, A.N. Starostin, K.R. Dezern, G.P. Tatsis and V.Y. Baranov, 1996. Microwave tomography: Two-dimensional system for biological imaging. *IEEE Trans. Biomed. Eng.*, 43: 869-877.
- Taflove, A., 1998. *Advances in Computational Electrodynamics: The Finite Difference Time Domain Method*. Artech House. Inc., 685 Canton Street, Norwood, MA 02062.